Call for Models—A Test Case for the Source Inversion Validation: The 2014 M_L 5.5 Orkney, South Africa, Earthquake

by Pamela A. Moyer, Margaret S. Boettcher, William L. Ellsworth, Hiroshi Ogasawara, Artur Cichowicz, Denver Birch, and Gerhard van Aswegen

ABSTRACT

We propose a test case for the Source Inversion Validation (SIV) community and other interested seismologists using high-quality waveforms of the M_L 5.5 Orkney, South Africa, earthquake. This rupture initiated ~5 km below the surface and terminated several hundred meters below the deepest levels of a gold mine. The Orkney earthquake and its aftershock sequence were well recorded by a dense network of surface and in-mine seismometers. *In situ* stress measurements and fault core through the rupture surface are anticipated to be available as part of the recently funded International Continental Scientific Drilling Program project to drill from within the mine into the Orkney earthquake rupture zone through a project titled “Drilling into Seismogenic Zones of M2.0-M5.5 Earthquakes in South African gold mines.” The remarkable quality and range of geophysical data available for the M_L 5.5 Orkney earthquake make this event an ideal test case for the SIV community using actual seismic data to determine the spatial and temporal evolution of earthquake rupture.

Electronic Supplement: Station locations and seismograms in ASCII format.

INTRODUCTION

Finite-fault source models describe the spatial and temporal evolution of earthquake rupture. There are many strategies to solve the inverse problem (e.g., Ide, 2007), but differences in data selection, processing methods, assumed geophysical parameters, and inversion techniques (Beresnev, 2003; Ide *et al.*, 2005) result in often-inconsistent rupture models (e.g., Mai and Thingbaijam, 2014). Most models are based on the representation theorem for seismic sources, which defines a linear relationship between the space- (y) and time- (τ) dependent displacement discontinuity across the fault surface $s(y, \tau)$ and the amplitude of the displacement wavefield $u(x, t)$ at position x and time t:

$$u(x, t) = \iint \mathbf{G}(y, t - \tau) s(y, \tau) dy d\tau \tag{1}$$

(Aki and Richards, 2002). The problem is discretized by replacing the fault surface with a grid of subfaults or other basis functions for which $\mathbf{G}$ is their impulse response seismogram at observation point x

$$\mathbf{u} = \mathbf{G}s + \mathbf{e}, \tag{2}$$

in which $\mathbf{u}$ is the data vector of the seismograms, $\mathbf{G}$ is the design matrix containing the synthetic seismograms for each source–station pair, s contains the unknown time history of the displacement discontinuity for each point source, and $\mathbf{e}$ is the error vector.

The Source Inversion Validation (SIV) project (Mai *et al.*, 2007; Page *et al.*, 2011; Mai, Schorlemmer, *et al.*, 2016) was developed to quantify the uncertainty in earthquake source inversions. This project provides statistical measures to rate models and offers forward modeling and benchmark exercises for testing methods (Mai, Schorlemmer, *et al.*, 2016). Inversion benchmarks as part of the SIV project (Mai, Schorlemmer, *et al.*, 2016) include datasets generated from rupture models that vary in complexity, ranging from spontaneous rupture on a dipping strike-slip fault to spatially varying rupture with more structural heterogeneity. Additional standards proposed by Mai, Shearer, *et al.* (2016) set guidelines for documenting the inversion process to promote transparency and reproducibly of results and facilitate their analysis and comparison. These standards recommend detailed descriptions of model parameters (including location, geometry, and slip history of each subfault), thorough documentation on data used in the inversion, and details on methods used to compute Green’s functions, data processing procedures, choice of priors, and preferred model misfit (Mai, Shearer, *et al.*, 2016). Up to now, the SIV

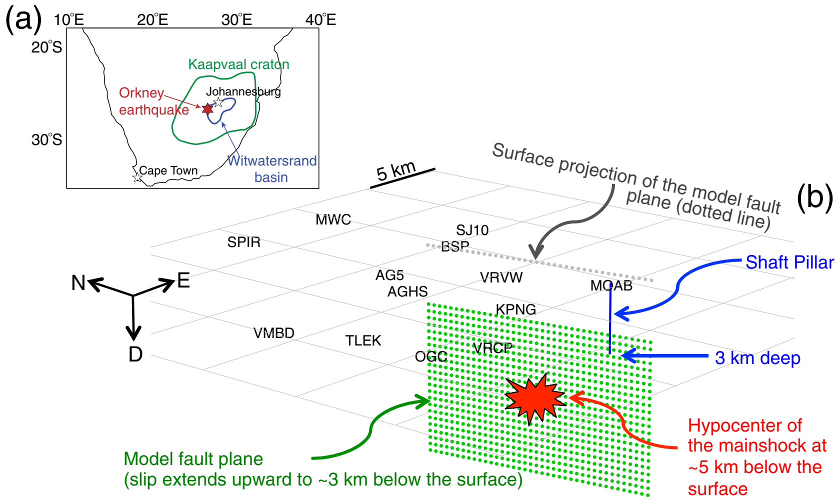

▲ **Figure 1.** (a) Geographic location and (b) surface seismic network and source geometry of the 2014 M_L 5.5 Orkney, South Africa, earthquake. The strike-slip rupture extended to a few hundred meters from the base of the mine and was recorded by dense surface and in-mine seismic networks. The color version of this figure is available only in the electronic edition.

community modeling exercises have only examined synthetic test cases.

On 5 August 2014, an M_L 5.5 earthquake occurred near a gold mine in Orkney, South Africa. This earthquake ruptured a near-vertical fault plane that extended ~7 km in depth and terminated upward, below the deepest mining levels, ~3 km below the surface (Imanishi *et al.*, 2016). In this article, depth is relative to the surface elevation of a local mine shaft collar that is 1310 m above mean sea level. The mine is located in the northwestern region of the Witwatersrand basin in the Kaapvaal craton, located ~160 km west-southwest of Johannesburg (Fig. 1). The region has been tectonically stable for the past two billion years (Kamo *et al.*, 1996) but has been modified through 5–10 km of erosion (McCarthy *et al.*, 1990). An immediate foreshock, the mainshock, and the aftershock sequence were recorded by a dense surface seismic network, in-mine seismometers, and strainmeters. In addition, the M_L 5.5 earthquake is the primary target of the recently initiated International Continental Scientific Drilling Program project "Drilling into Seismogenic Zones of M2.0-M5.5 Earthquakes in South African gold mines" (DSeis; Ogasawara *et al.*, 2017). With abundant high-quality waveforms, *in situ* stress measurements, and the anticipated DSeis logging and fault core data to constrain the rupture process, this earthquake is an ideal test case for the SIV community and provides an opportunity to use actual seismic data as an inversion benchmark.

DATA

The South African Council for Geoscience (CGS) operates a national network of 26 broadband seismometers distributed across South Africa and three clusters of strong ground motion sensors, including one broadband sensor, within 200 km of the M_L 5.5 Orkney earthquake (Midzi *et al.*, 2015). The network cluster near the mainshock epicenter provides continuous recording at 200-Hz sample rate from 15 seismometers (Fig. 1). The CGS recordings (freely available online), as well as proprietary data recorded in trigger mode on underground seismometers and underground strainmeters, provided excellent azimuthal recording coverage of the earthquake sequence. The mainshock surface recordings from the CGS network exhibit high signal-to-noise ratio and integrate well to displacement (Fig. 2). Near-field terms can be seen on the displacement seismograms, including ramps between *P* and *S* (e.g., Fig. 2a,b,f) and permanent displacement offsets (e.g., Fig. 2e). The mainshock exhibits a complex rupture, which includes a slow initiation observed as a foreshock preceding the mainshock by ~1 s. The foreshock *S* wave is lost in the *P*-wave coda at most of the nearby surface stations.

The M_L 5.5 Orkney earthquake was a strike-slip earthquake that produced higher than expected ground motion, given its epicentral distance (Council for Geoscience, 2014), and resulted in local damage. More than 400 aftershocks were recorded by surface seismometers in the day following the mainshock (Midzi *et al.*, 2015), and their spatial distribution delineated a nearly vertical mainshock fault plane between ~4–7 km depth and strike north-northwest–south-southeast (Imanishi *et al.*, 2016). The model fault plane shown in Figure 1, with parameters given in Table 1, approximates the source plane delineated with the aftershock distribution.

We constrained hypocentral depths of local earthquakes using both in-mine and surface station recordings. VELEST (Kissling *et al.*, 1994, 1995) was used for the simultaneous inversion of *P*- and *S*-wave travel times to obtain initial *P*- and *S*-wave velocity models, station corrections, origin times, and earthquake hypocentral depths. Arrival times for 12 of the largest ($M_L \geq 2.0$) earthquakes near the mainshock epicenter were used in the inversion (Table 2), including 336 *P* arrivals and 296 *S* arrivals. Earthquake depths were constrained to between 1.65 and 4.29 km below the surface.

A simple two-layer velocity model (Table 3) was developed from the surface recordings of local earthquakes. Travel times and hypocentral depths obtained from VELEST were used to calculate travel-time curves, from which we determined the velocity model given in Table 3. Travel times for one earthquake, as observed at surface stations, are shown in Figure 3. The model consists of a 1.4-km-thick surface layer with a *P*-wave velocity of $V_P = 3.8$ km/s and an *S*-wave velocity of $V_S = 2.3$ km/s. Below the surface layer is a layer with $V_P = 5.8$ km/s and $V_S = 3.5$ km/s that extends to depth. Travel times from in-mine stations, most located ~1–3 km below the surface, are fit well by a uniform velocity model with $V_P = 5.8$ km/s and $V_S = 3.5$ km/s. No change in residuals is observed for shallow versus deep travel paths, validating the velocities in

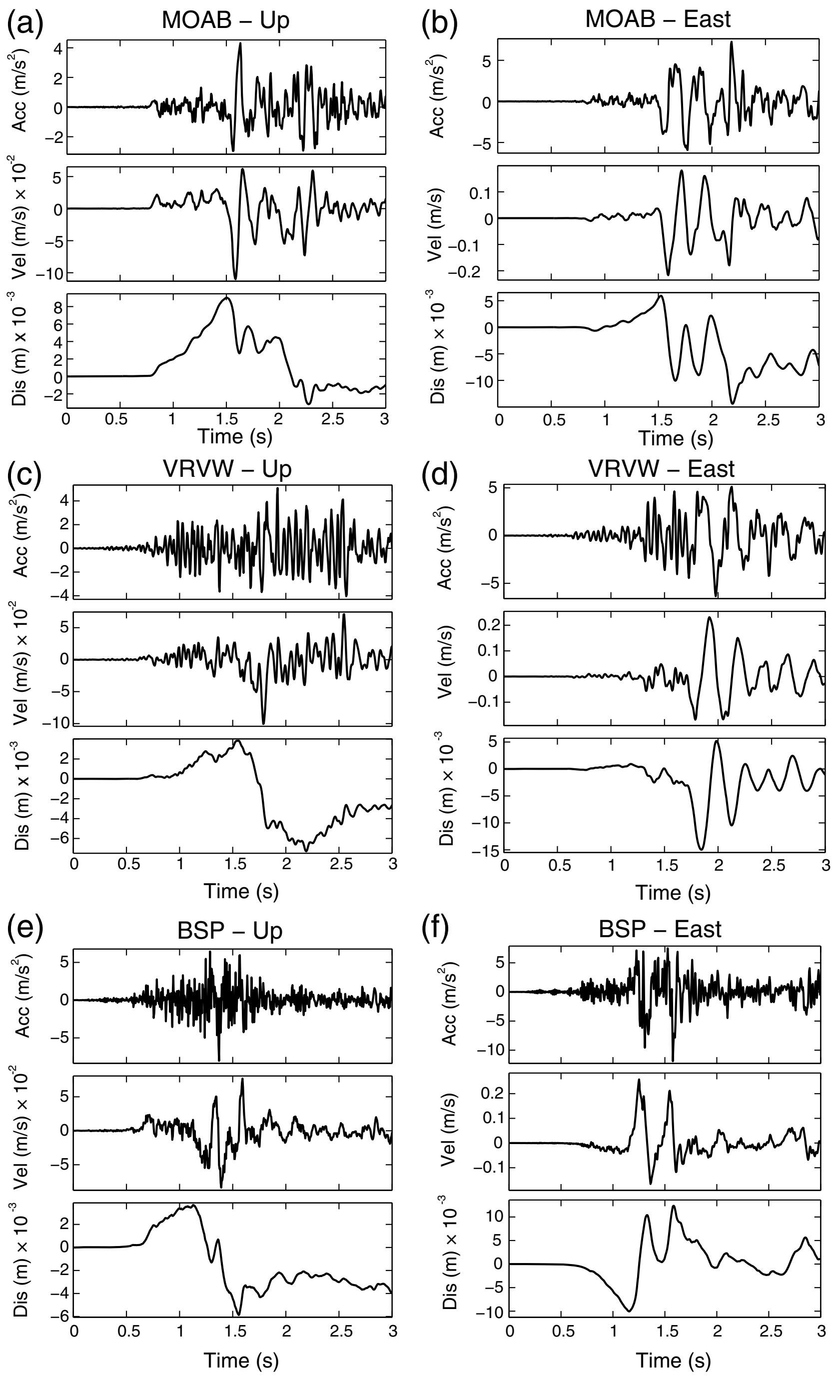

▲ **Figure 2.** Example vertical- and east-component acceleration (Acc), velocity (Vel), and displacement (Dis) seismograms from three surface stations. Each record starts at the *P*-wave arrival for the foreshock, ~1 s prior to the M_L 5.5 mainshock. Note the near-field terms, including the permanent offsets seen on the vertical component of (c) VRVW and (e) BSP and the ramps between *P*- and *S*-wave arrivals seen on both components of (a,b) MOAB and (e,f) BSP.

the deeper layer. The *P*- and *S*-wave velocities obtained from VELEST for the deeper layer are typical for surrounding mines, which have $V_P = 5.9$ km/s and $V_S = 3.6$ km/s and a crustal density representative for the area of 2640 kg/m^3 (Boettcher *et al.*, 2015).

CONTRIBUTION TO THE SOURCE INVERSION VALIDATION (SIV) PROJECT

We invite the source inversion community to model the 2014 M_L 5.5 Orkney earthquake as a comparison exercise. We anticipate comparing slip models using methods developed in previous SIV exercises as part of a Southern California Earthquake Center workshop. Anyone interested in participating in this workshop or with questions should contact the authors for more information. Seismic data from surface stations are available as recorded directly from the CGS in South Africa or as processed to acceleration, velocity, or displacement (see Ⓔ electronic supplement available to this article and Fig. 2). Earthquakes used in the hypocenter and velocity inversion (Table 2) are available online from CGS and may also be suitable as empirical Green's functions (see Data and Resources). The proprietary in-mine seismograms are reserved for blind testing.

More specifically, we request that source modeling teams submit kinematic slip histories following the onset of the immediate foreshock to the SIV benchmark platform (see Data and Resources). Our preferred hypocenter location and an initial fault-plane orientation are given in Table 1, but modeling teams are welcome to use any hypocenter and fault model in solving for the displacement time history. We request that each modeling team submit synthetic three-component seismograms for the locations of five in-mine seismometers (see Ⓔ Table S2). We will use these synthetic seismograms for blind testing with the observed in-mine-recorded waveforms.

We plan to use quantitative analysis tools provided by the SIV platform, including FORTRAN programs and related MATLAB scripts from Kristekova *et al.* (2009) to compare submitted inversion solutions with the actual data. These tools implement misfit measurements of the waveform (L1 and L2 norms, variance reduction, and cross correlation), time–frequency envelope, and time–frequency phase to statistically evaluate the goodness of fit (Kristekova *et al.*, 2009; Mai, Schorlemmer, *et al.*, 2016). Solutions should be submitted using the recommended formats for rupture models, ground motions, and displacements as described at the SIV benchmark platform (see Data and Resources). As recommended by previous SIV efforts (Mai, Schorlemmer, *et al.*, 2016), participants are expected to submit with their solutions all seismic phases that were modeled and all seismic stations

Table 1
Initial Source Information for the 2014 M_L 5.5 Orkney Earthquake

	Foreshock	Mainshock
Latitude (°)	−26.9525	−26.9401
Longitude (°)	26.8151	26.8125
Depth below the surface (km)*	5.14	4.87
Origin time (UTC)	2014/08/05 10:22:34.01	2014/08/05 10:22:35.61
Fault plane (approximate)		
Strike (°)	351	351
Dip (°)	90	90
Rake (°)	0	0

*Depth is relative to the surface elevation of a local mine-shaft collar, which is 1310 m above mean sea level.

that were used, including the station names, components, waveform types (acceleration, velocity, displacement), and filter parameters.

The proposed workshop will intercompare participant solutions and predicted seismograms using the SIV methodologies. The DSeis project will collect physical samples of the fault rupture, along with physical properties of the fault zone (fracture density, damage state, etc.). By combining kinematic and/or dynamic models of the faulting at the location of the fault penetration by the drill hole, we have an opportunity to go far beyond the conventional interpretation and limitations of previous source inversion models.

SUMMARY

The 2014 M_L 5.5 Orkney earthquake provides a unique opportunity to directly compare seismological inferences with deep *in situ* observations of faulting. Well-constrained geophysical data and high-quality waveforms make this earthquake an ideal test case for the SIV community. Actual seismic data, as opposed to synthetic data, are now available to test the reliability and robustness of source inversion models. Anyone interested in participating in an SIV workshop using seismic data from the Orkney earthquake, or with questions regarding the workshop or data, should contact the authors for more information.

DATA AND RESOURCES

Seismic data for the M_L 5.5 Orkney earthquake from the closest 15 surface stations are available in the Ⓔ electronic

Table 2
Origin Times and Hypocenters for Earthquakes Used in the Velocity Model Inversion

Event	Origin Time (yyyy/mm/dd hh:mm:ss.ss)	M_L	Latitude (°)	Longitude (°)	Depth (km)*
1	2014/08/05 17:29:51.39	2.0	−26.9474	26.8026	1.76
2	2014/08/05 22:55:18.05	2.1	−26.9764	26.8122	3.95
3	2014/08/06 00:43:52.33	2.4	−26.9830	26.8135	4.18
4	2014/08/06 02:01:38.48	2.9	−26.9754	26.8122	3.86
5	2014/08/08 07:16:41.17	2.0	−26.9813	26.8129	4.20
6	2014/08/09 14:31:21.26	2.3	−26.9830	26.8141	4.29
7	2014/08/27 23:18:56.06	3.4	−26.9513	26.8060	1.65
8	2014/09/02 16:22:15.17	2.1	−26.9790	26.8289	2.45
9	2014/09/04 09:30:29.11	2.5	−26.9442	26.8059	2.17
10	2014/09/09 19:46:47.12	2.4	−26.9882	26.8153	4.20
11	2014/10/12 11:27:38.33	2.0	−26.9912	26.8160	3.86
12	2014/10/28 12:57:54.39	2.6	−26.9886	26.8155	3.94

*Depth is relative to the surface elevation of a local mine-shaft collar, which is 1310 m above mean sea level.

Table 3
One-Dimensional Velocity Model for the 2014 M_L 5.5 Orkney Earthquake

Layer	Depth at Top of Layer (km)*	V_P (km/s)	V_S (km/s)	V_P/V_S
1	0	3.8	2.3	1.65
2	1.4	5.8	3.5	1.65

*Depth is relative to the surface elevation of a local mine-shaft collar, which is 1310 m above mean sea level.

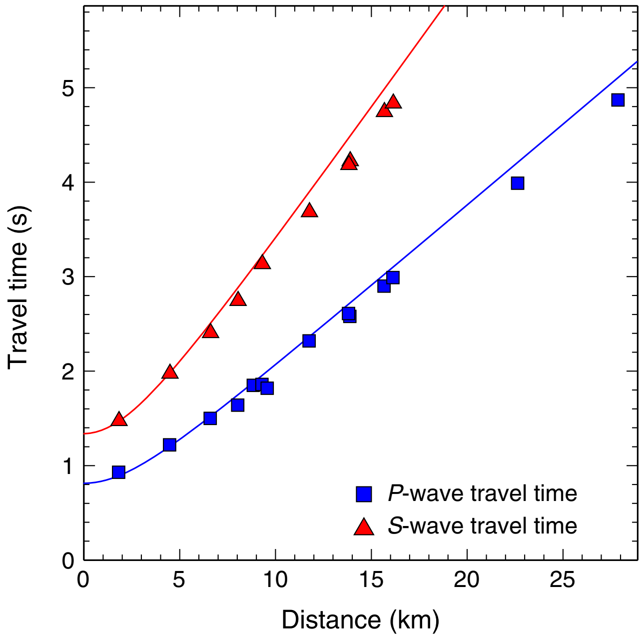

▲ **Figure 3.** Travel-time curve (Table 2, event 2) using travel times and hypocentral depths obtained from VELEST to determine a velocity model for the 2014 M_L 5.5 Orkney earthquake. The data are fit well by the velocity model given in Table 3, which describes a 1.4-km-thick surface layer with $V_P = 3.8$ km/s and $V_S = 2.3$ km/s over a layer with $V_P = 5.8$ km/s and $V_S = 3.5$ km/s that extends to depth. The color version of this figure is available only in the electronic edition.

supplement as ASCII files: three-component (north, east, and vertical) seismograms in acceleration, velocity, and displacement. Seismic data for the mainshock and the 12 aftershocks listed in Table 2 may also be obtained directly from the Council for Geoscience (CGS) at http://geoscience.org.za/index.php/seismic-events/125-5-8august-2014-orkney-event/438-5-august-2014-160%20orkney-event (last accessed June 2017). Information on the Source Inversion Validation (SIV) project, including benchmark exercises and recommended file formats for solutions, can be found at http://equake-rc.info/SIV/ (last accessed June 2017). The MATLAB software is available from MathWorks at https://www.mathworks.com/products/matlab (last accessed June 2017)

ACKNOWLEDGMENTS

We gratefully acknowledge assistance from the South African Council for Geosciences (CGS) and AngloGold Ashanti for access to seismic data and geophysical information. We thank Kazutoshi Imanishi for sharing his analysis of the hypocenter of the M_L 5.5 mainshock and thank the "Drilling into Seismogenic Zones of M2.0-M5.5 Earthquakes in South African gold mines" (DSeis)-International Continental Scientific Drilling Program (ICDP) team and ICDP and DSeis workshop in Potchefstroom, South Africa, for making this work possible. We also thank Zhigang Peng, Martin Mai, and an anonymous reviewer for their insightful and instructive comments that greatly improved this article. This project was supported by the Southern California Earthquake Center (SCEC) Award Number 16159 to W. E. and M. B.

REFERENCES

Aki, K., and P. Richards (2002). *Quantitative Seismology*, Second Ed., University Science Books, Sausalito, California.

Beresnev, I. A. (2003). Uncertainties in finite-fault slip inversions: To what extent to believe? (A critical review), *Bull. Seismol. Soc. Am.* **93,** 2445–2458, doi: 10.1785/0120020225.

Boettcher, M. S., D. L. Kane, A. McGarr, M. J. S. Johnston, and Z. Reches (2015). Moment tensors and other source parameters of mining-induced earthquakes in TauTona Mine, South Africa, *Bull. Seismol. Soc. Am.* **105,** 1576–1593, doi: 10.1785/0120140300.

Council for Geoscience (CGS) (2014). Report on the recommendations for the magnitude 5.5 earthquake on 5 August 2014 in Klerksdrop-Orkney region, *Report Number 2014–0277*.

Ide, S. (2007). Slip inversion, in *Treatise on Geophysics*, G. Schubert (Editor), in Earthquake Seismology, H. Kanamori (Editor), Vol. 4, Elsevier, Amsterdam, The Netherlands, 193–224, ISBN: 978-0-444-51932-0.

Ide, S., G. C. Beroza, and J. J. McGuire (2005). Imaging earthquake source complexity, in *Seismic Earth: Array Analysis of Broadband Seismograms*, A. Levander and G. Nolet (Editors), AGU, Washington, D.C.

Imanishi, K., H. Ogasawara, Y. Yabe, S. Horiuchi, M. Okubo, and O. Murakami (2016). Aftershock distribution and focal mechanisms of 2014 M_w 5.4 Orkney earthquake, South Africa, by using underground seismic networks in gold mines, *JpGU Meeting*, Abstract SSS27–17.

Kamo, S. L., W. U. Reimold, T. E. Krogh, and W. P. Colliston (1996). A 2.023 Ga age for the Vredefort impact event and a first report of shock metamorphosed zircons in pseudotachylitic breccias and granophyres, *Earth Planets Space* **144,** nos. 3/4, 369–387, doi: 10.1016/S0012-821X(96)00180-X.

Kissling, E., W. L. Ellsworth, D. Eberhart-Phillips, and U. Kradolfer (1994). Initial reference models in local earthquake tomography, *J. Geophys. Res.* **99,** 19,635–19,646.

Kissling, E., U. Kradolfer, and H. Maurer (1995). *Program VELEST User's Guide—Short Introduction (Second Draft Version)*, Institute of Geophysics and Swiss Seismological Service, ETH-Hoenggerberg, Zurich, Switzerland, 1–26.

Kristekova, M., J. Kristek, and P. Moczo (2009). Time–frequency misfit and goodness-of-fit criteria, *Geophys. J. Int.* **178,** 813–825, doi: 10.1111/j.1365-246X.2009.04177.x.

Mai, P. M., and K. K. S. Thingbaijam (2014). SRCMOD: An online database of finite source rupture models, *Seismol. Res. Lett.* **85,** 1348–1357, doi: 10.1785/0220140077.

Mai, P. M., J. Burjanek, B. Delouis, G. Festa, C. Francois-Holden, D. Monelli, T. Uchide, and J. Zahradnik (2007). Earthquake source inversion blindtest: Initial results and further developments, *Eos Trans. AGU* **88,** no. 52 (Fall Meet. Suppl.), Abstract S53C–08.

Mai, P. M., D. Schorlemmer, M. Page, J.-P. Ampuero, K. Asano, M. Causse, S. Custodio, W. Fan, G. Festa, M. Galis, *et al.* (2016). The earthquake-Source Inversion Validation (SIV) project, *Seismol. Res. Lett.* **87,** no. 3, 690–708, doi: 10.1785/0220150231.

Mai, P. M., P. Shearer, J.-P. Ampuero, and T. Lay (2016). Standards for documenting finite-fault earthquake rupture models, *Seismol. Res. Lett.* **87,** no. 3, 712–718, doi: 10.1785/0220150204.

McCarthy, T. S., I. G. Stanistreet, and L. J. Robb (1990). Geological studies related to the origin of the Witwatersrand basin and its mineralization: An introduction and a strategy for research and exploration, *S. Afr. J. Geol.* **93,** 1–4.

Midzi, V., B. Zulu, B. Manzunzu, T. Mulabisana, T. Pule, S. Myendeki, and W. Gubela (2015). Macroseismic survey of the M_L 5.5, 2014 Orkney earthquake, *J. Seismol.* **19,** 741, doi: 10.1007/s10950-015-9491-2.

Ogasawara, H., Y. Yabe, T. Ito, G. van Aswegen, A. Cichowicz, R. Durrheim, T. Onstott, T. Keift, A. Ishida, H. Y. Ogasawara, *et al.* (2017). Drilling to probe quasi-static and dynamic seismic ruptures in deep South African gold mines (DSeis) from cm- to km-scale, *Schatzalp 2nd Induced Seismicity Workshop*, Davos, Switzerland, 14–17 March, available at http://www.seismo.ethz.ch/export/sites/sedsite/research-and-teaching/.galleries/pdf_schatzalp/1_Schatzalp2017_Ogasawara.pdf (last accessed June 2017).

Page, M., P. M. Mai, and D. Schorlemmer (2011). Testing earthquake source inversion methodologies, *Eos Trans. AGU* **92,** no. 9, 75.

Pamela A. Moyer
Margaret S. Boettcher[1]
Department of Earth Sciences
University of New Hampshire
56 College Road
James Hall Room 214
Durham, New Hampshire 03824 U.S.A.
Pamela@PamelaMoyer.net

William L. Ellsworth
Department of Geophysics
Stanford University
397 Panama Mall
Mitchell Building Room 373B
Stanford, California 94305 U.S.A.

Hiroshi Ogasawara
College of Science and Engineering
Ritsumeikan University
1-1-1 Noji Higashi
Kusatsu 525-8577, Japan

Artur Cichowicz
Mine Seismology Consultancy
Magnoli 6/4
05-500 Warsaw
Poland

Denver Birch
Gerhard van Aswegen
Council for Geoscience
280 Pretoria Street
Silverton, Pretoria 0001
South Africa

Published Online 5 July 2017

[1] Also at School of Earth and Environment, The University of Western Australia, 35 Stirling Highway, Perth, Western Australia 6009, Australia.